N-Myristoylethanolamine–cholesterol (1:1) complex: first evidence from differential scanning calorimetry, fast-atom-bombardment mass spectrometry and computational modelling

M. Ramakrishnan, Roopa Kenoth, Ravi Kanth Kamlekar, M. Sharath Chandra, T.P. Radhakrishnan, Musti J. Swamy*

School of Chemistry, University of Hyderabad, Hyderabad 500 046, India

Received 21 August 2002; revised 2 October 2002; accepted 3 October 2002

First published online 17 October 2002

Edited by Guido Tettamanti

Abstract The interaction of *N*-myristoylethanolamine (NMEA) with cholesterol is investigated by differential scanning calorimetry (DSC), fast-atom-bombardment mass spectrometry (FAB-MS) and computational modelling. Addition of cholesterol to NMEA leads to a new phase transition at 55°C besides the chain-melting transition of NMEA at 72.5°C. The enthalpy of the new transition increases with cholesterol content up to 50 mol%, but decreases thereafter, vanishing at 80 mol%. The enthalpy of the chain-melting transition of NMEA decreases with an increase in cholesterol; the transition disappears at 50 mol%. FAB-MS spectra of mixtures of NMEA and cholesterol provide clear signatures of the formation of {[NMEA+cholesterol]$^+$} {[NMEA+cholesterol+Na]$^+$}. These results are consistent with the formation of a 1:1 complex between NMEA and cholesterol. Molecular modelling studies support this experimental finding and provide a plausible structural model for the complex, which highlights multiple H-bond interactions between the hydroxy group of cholesterol and the hydroxy and carbonyl groups of NMEA besides appreciable dispersion interaction between the hydrocarbon domains of the two molecules.

Key words: Biomembrane; Hydrogen bonding; Differential scanning calorimetry; Fast-atom-bombardment mass spectrometry; Computational modelling

1. Introduction

Long-chain *N*-acylethanolamines (NAEs) [1] and their precursors, *N*-acylphosphatidylethanolamines, play vital roles in a variety of biological processes. They accumulate in plants and animals during stress conditions such as injury or dehydration, rising to very high levels when extensive membrane degradation such as in myocardial infarction are encountered [1–7]. *N*-Arachidonylethanolamine (anandamide) acts as an endogenous ligand of the type-I cannabinoid receptors, inhibits gap–junction conductance and reduces the fertilizing capacity of the sperm [8–10]. *N*-Palmitoylethanolamine is an endogenous ligand for type-II cannabinoid receptors [11]. *N*-Myristoylethanolamine (NMEA) and *N*-lauroylethanolamine are secreted into the culture medium of tobacco cells when challenged by the fungal elicitor, xylanase; however, the underlying mechanism of this process is still not clear [12,13]. The anti-inflammatory, antibacterial and antiviral properties of NAEs are of considerable application potential [1].

In order to develop structure–function relationships for NAEs, it is essential to characterize their physical properties and interaction with other membrane constituents such as cholesterol, phospholipids and integral membrane proteins. In earlier studies the phase transitions of a homologous series of NAEs were characterized by differential scanning calorimetry and the molecular packing and intermolecular interactions of NMEA were investigated by single-crystal X-ray diffraction [14–16]. It was observed that NMEA molecules pack in a bilayer format, analogous to that found in phospholipid membranes [16]. This report presents the results of differential scanning calorimetry (DSC) and fast-atom-bombardment mass spectrometry (FAB-MS) complemented by computational modelling which provide the first evidence for a 1:1 complexation between NMEA and cholesterol.

2. Materials and methods

2.1. Materials

N-Myristoylethanolamine was synthesized and characterized as described earlier [14]. Cholesterol was purchased from Avanti Polar Lipids (Alabaster, AL, USA).

2.2. Differential scanning calorimetry

Mixtures of NMEA and cholesterol were prepared by mixing appropriate volumes of the two lipids from stock solutions in dichloromethane. The solvent was removed under a stream of dry N_2 gas, followed by vacuum desiccation for 3 h. Dry samples of NMEA, cholesterol and their mixtures were weighed accurately using a Perkin-Elmer Cahn microbalance into stainless steel pans, 30 μl of double distilled water was added, and the pans were sealed. DSC measurements were performed on a Perkin-Elmer DSC-4 calorimeter equipped with a data station. The samples were hydrated by incubation at 90°C for 30 min in the calorimeter and then cooled to 35°C. After incubation at this temperature for 20 min, two heating scans and one cooling scan were recorded at a scan rate of 2.5°/min. After each scan, the sample was incubated for 10 min at the final temperature of the scan. Transition enthalpies were evaluated by integrating the area under each peak using the software supplied by the instrument manufacturers.

2.3. Fast-atom-bombardment mass spectrometry

FAB mass spectra were recorded on an Autospec (Micromass,

*Corresponding author. Fax: (91)-40-301 2460 or 0145.
E-mail address: mjssc@uohyd.ernet.in (M.J. Swamy).

0014-5793/02/$22.00 © 2002 Published by Elsevier Science B.V. on behalf of the Federation of European Biochemical Societies.
PII: S0014-5793(02)03553-6

Manchester, UK) mass spectrometer using an OPUS V3.IX data system [17].

2.4. Computational methodology

Molecular modelling studies were carried out using a combination of empirical force field available in the MOE program and the AM1 semi-empirical quantum chemical method. The MOE program (Molecular Operating Environment, Version 2001.01) is available from Chemical Computing Group (1010 Sherbrooke Street West, Montreal, Canada H3A 2R7; website: http://www.chemcomp.com). AM1 computations were carried out using the MOPAC93 program (©Fujitsu, Japan). Geometries of NMEA and cholesterol were optimized using the empirical potentials followed by the AM1 method. Default options in MOE were employed in systematic conformational search on conformations arising out of bond rotations at 10° intervals in the hydrophilic region of NMEA. In optimizations of the complex using the 'water soak' option of MOE, 339 water molecules in the default layer width and box metric were used and PEOE (partial equalization of orbital electronegativities) electrostatic charges were computed for all atoms and included.

3. Results and discussion

3.1. Differential scanning calorimetry

Heating thermograms of hydrated samples of NMEA, cholesterol and their mixtures are shown in Fig. 1. Consistent with earlier results, hydrated NMEA shows a reversible, highly cooperative gel-fluid chain-melting phase transition centered at 72.5°C [14]. Addition of cholesterol at low mole fractions results in two distinct changes in the thermograms. First, the intensity of the peak corresponding to the chain-melting transition decreases with slight broadening. In addition, a second peak appears around 55°C, indicating a new phase transition. The intensity of this peak increases with increasing NMEA:cholesterol ratio up to 1:1 (mol/mol), whereas the intensity of the peak corresponding to the chain-melting of NMEA decreases steadily and disappears completely at the same ratio. Intensity of the peak at 55°C also decreases with increasing cholesterol content and becomes nearly zero at 0.8 mole fraction of the sterol. Cooling scans indicate that both the transitions are reversible. Pure cholesterol does not show any phase transition between 35 and 90°C (data shown between 50 and 80°C in Fig. 1).

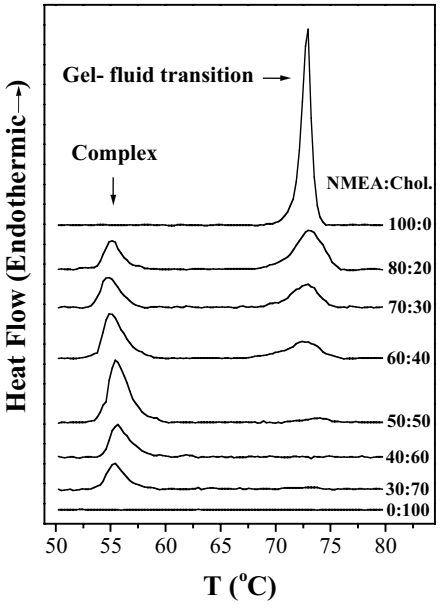

Fig. 1. Representative heating thermograms of aqueous dispersions of NMEA, cholesterol and their mixtures. The composition of the lipid mixtures (in mol ratio) is indicated. Scan rate is 2.5°/min. The *y*-scale is not the same for all the scans shown.

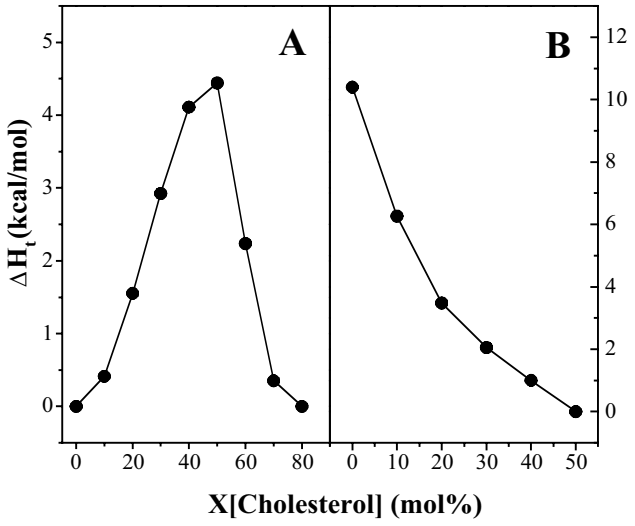

Fig. 2. Plot of the change in transition enthalpy (ΔH_t) as a function of cholesterol composition for hydrated mixtures of NMEA and cholesterol. A: Transition corresponding to the 1:1 complex. B: Transition corresponding to the chain-melting of NMEA. Transition enthalpies in A were calculated using the weighted average of the molecular weights of NMEA and cholesterol, whereas those in B were calculated based on the molecular weight of NMEA alone.

A plot depicting the variation of the change in enthalpy (ΔH_t) of the two transitions as a function of the cholesterol content in the mixture is given in Fig. 2. For the transition at 55°C, ΔH_t increases gradually up to 50 mol% cholesterol and then decreases steadily and reaches a value of zero at 80 mol% cholesterol. ΔH_t values corresponding to the chain-melting transition of NMEA decrease monotonically with increasing cholesterol content and approach zero at 50 mol% cholesterol. These results suggest the formation of a 1:1 complex between NMEA and cholesterol. The thermograms indicate the coexistence of the complex and NMEA in the mixtures containing < 50 mol% cholesterol, and the complex and pure cholesterol in the mixtures containing > 50 mol% cholesterol. The mixture having 50 mol% cholesterol contains the complex exclusively.

3.2. Fast-atom-bombardment mass spectrometry

In order to further investigate the interaction between NMEA and cholesterol, we carried out fast-atom-bombardment mass spectrometric studies. Due to the soft ionization technique employed, FAB-MS is particularly suited for the investigation of complexes that are held by relatively strong hydrogen bonds [18–20]. FAB mass spectrum of a 1:1 (mol/mol) mixture of NMEA and cholesterol, prepared in the same manner as for the DSC studies, is given in Fig. 3. The relative intensity and peak assignment data are given in Table 1. Peaks corresponding to NMEA are prominently seen at *m*/*z* values of 272 $\{[M+H]^+\}$, 294 $\{[M+Na]^+\}$; peaks corresponding to $(NMEA)_2$ are also seen with moderate intensity at *m*/*z* value of 544 $\{[M_2+H]^+\}$ and 566 $\{[M_2+Na]^+\}$. The low intensity peaks at 387 $\{[M+H]^+\}$ and 369 $\{[M-OH]^+\}$ correspond to cholesterol. Most interestingly, peaks are observed

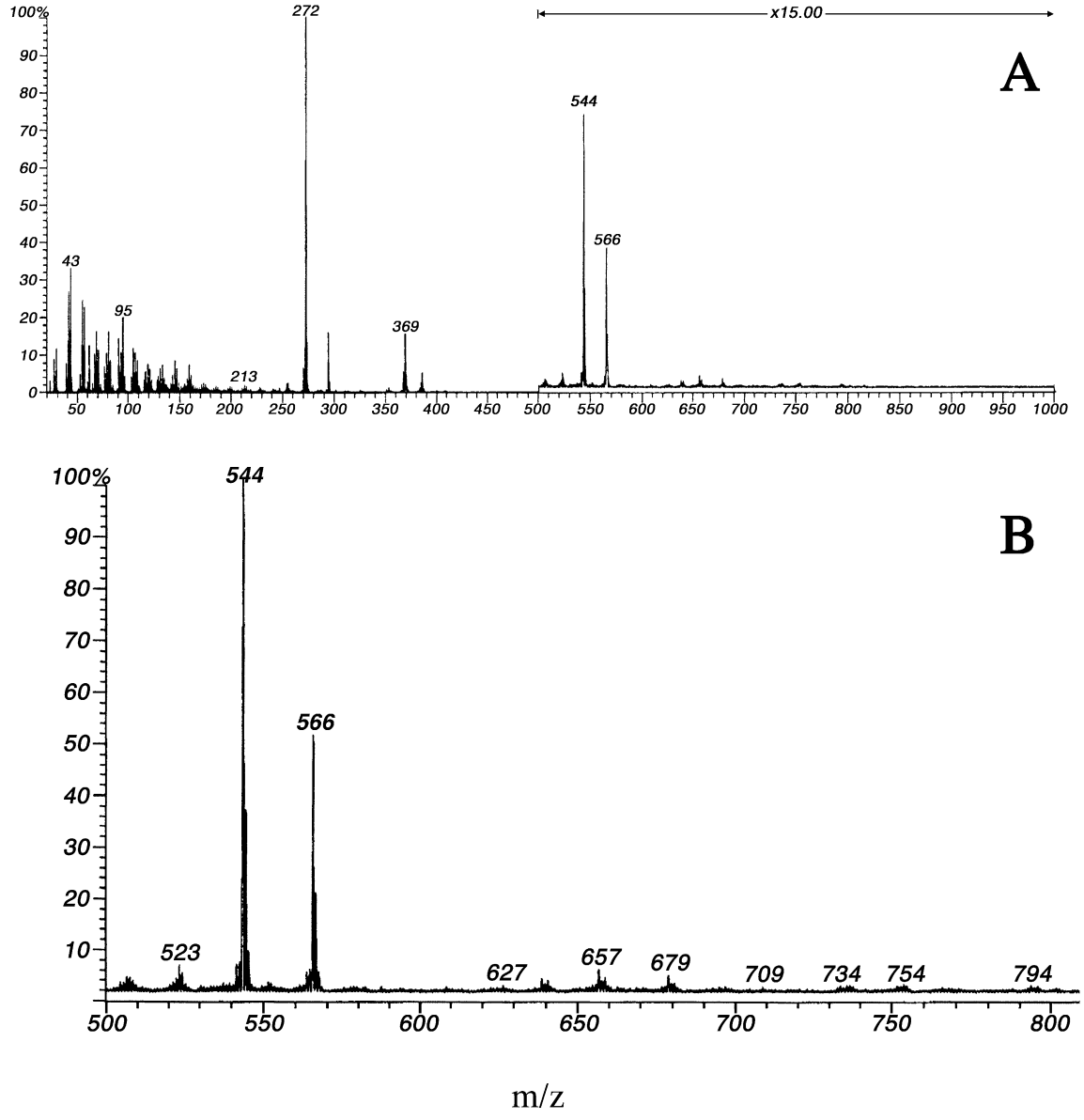

Fig. 3. Fast-atom-bombardment mass spectrum of a 1:1 (mol/mol) mixture of NMEA and cholesterol. A: Spectrum in the *m/z* range 20–1000. B: Expanded spectrum in the *m/z* range 500–800.

at significantly higher masses, especially at *m/z* values of 657 and 679; these are clearly assignable to [NMEA+cholesterol+H]$^+$ and [NMEA+cholesterol+Na]$^+$. Though the relative abundances of these peaks are rather low compared to the base peak (*m/z* = 272), they are quite appreciable (5.6% and 4.6%, respectively) when compared to the intensity of the molecular ion of cholesterol. Their intensities compare quite favorably with the relative abundances of 4.9% and 2.5% observed for the peaks at *m/z* values of 544 and 566, corresponding to {[(NMEA)$_2$+H]$^+$} and {[(NMEA)$_2$+Na]$^+$}, respectively. Finally, no peaks corresponding to cholesterol dimer are observed in these spectra. These data clearly indicate that even after ionization, NMEA and cholesterol exist as a complex. Additionally, very similar mass spectrum (not shown) was obtained when solid samples of the two species were mixed directly in the probe tip of the mass spectrometer, suggesting that NMEA and cholesterol form a complex even in the gas phase.

An extended H-bond network mediated by hydroxy, amino and carbonyl functionalities is observed in the NMEA crystal [16]. Therefore, it is very likely that NMEA and cholesterol bind together to form the complex, using multiple strong

Table 1
Data from positive ion FAB-MS of NMEA-cholesterol (1:1, mol/mol) mixture

m/z	Relative intensity	Assignment
272	100.00	(NMEA+H)$^+$
294	15.70	(NMEA+Na)$^+$
369	15.70	(Chol.−OH)$^+$
387	5.20	(Chol.+H)$^+$
544	4.90	(NMEA$_2$+H)$^+$
566	2.50	(NMEA$_2$+Na)$^+$
639	0.22	(NMEA+Chol.−OH)$^+$
657	0.29	(NMEA+Chol.+H)$^+$
679	0.24	(NMEA+Chol.+Na)$^+$

H-bond interactions. The FAB-MS results are fully consistent with such a view.

3.3. Molecular modelling

Molecular modelling combining empirical force field and semi-empirical quantum chemical AM1 computations strongly support the DSC and FAB-MS evidence presented above for the formation of a 1:1 stoichiometric complex between NMEA and cholesterol and provide a plausible structural model for it. Geometries of NMEA and cholesterol were optimized using empirical potentials; the NMEA structure obtained through a stochastic followed by a systematic conformational search agrees well with the one obtained from the crystal structure analysis [16]. The two molecules were oriented appropriately to facilitate H-bond interaction between their hydrophilic groups; suitable and minimal bond rotations in the hydrophilic regions of the two molecules were effected for this purpose. An extensive set of initial geometries of the complex was then examined through full geometry optimization using the AM1 method employing the PRECISE conditions. Alternately, the initial geometries were optimized under the 'water soak' option of MOE followed by AM1 optimization. The low energy optimized structures of the complex showed significant H-bond interactions between the hydroxy group of cholesterol and the hydroxy and carbonyl groups of NMEA. The lowest energy structure obtained in our computations is shown in Fig. 4. Two prominent H-bond interactions, one between the hydroxy group of cholesterol and the carbonyl group of NMEA ($r_{H..O} = 2.21$ Å, $\theta_{O-H..O} = 135.0°$), and the other formed by the hydroxy groups of NMEA and cholesterol ($r_{H..O} = 2.16$ Å, $\theta_{O-H..O} = 157.5°$), lead to the cyclic formation, which can be represented as r_2^2 (9), in graph set

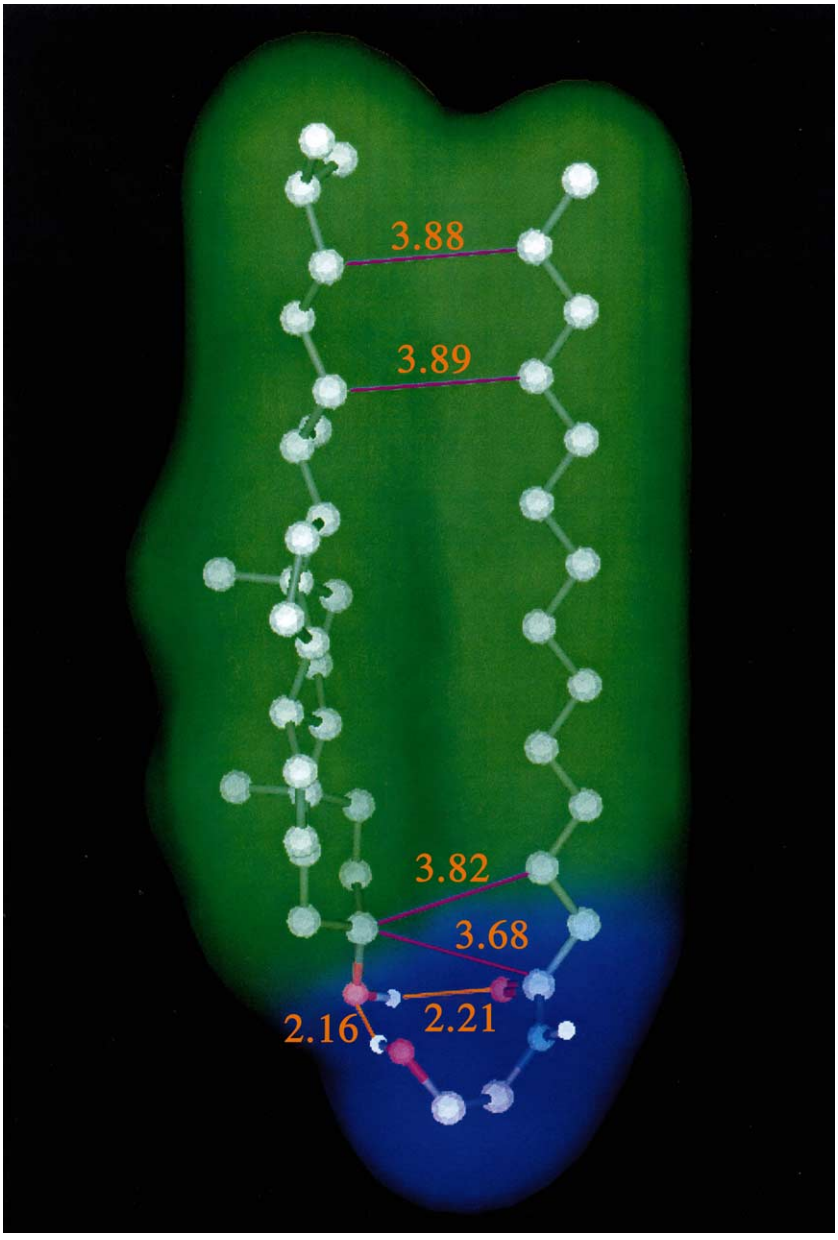

Fig. 4. AM1 optimized structure of the cholesterol–NMEA complex. Non-polar H atoms are omitted for clarity. The hydrophilic (blue) and hydrophobic (green) regions are represented using the Gauss–Connolly molecular surface computed using the default options in MOE. Orange lines represent short intermolecular H-bonds and violet lines indicate the non-bonded C...C contacts; the distances shown are in Å.

notation [21]. Interestingly, the optimized geometry of the complex also reveals appreciable dispersion interaction between the hydrocarbon domains of the two molecules as seen from several close C...C contacts, the lowest ones ranging from 3.68 Å to 3.89 Å. Fig. 3 emphasizes the hydrophobic and hydrophilic regions of the complex resulting from the various intermolecular interactions. The model structure of the complex illustrates a close matching of the size and hydrophilic/hydrophobic regions of the partner molecules leading to a compact pairing. The enthalpies of formation of the fully AM1 optimized geometries of the complex, NMEA and cholesterol indicate an appreciable stabilization of 5.3 kcal/mol for the complex. If the nearest local minima of cholesterol and NMEA, obtained by optimization starting from their respective geometries in the complex, are used, the stabilization of the complex increases to 6.9 kcal/mol.

3.4. Functional implications

Cholesterol is a ubiquitous plasma membrane lipid and its interaction with different phospholipids and sphingolipids has been the subject of numerous studies [22,23]. During the last decade there has been a renewed interest in understanding the interaction of cholesterol with other lipids in view of its presence in membrane *rafts*, which are rich in cholesterol and sphingolipids, resulting in the identification of novel 'condensed complexes' between cholesterol and phospholipids with simple integral stoichiometry [24–30]. These complexes have been implicated in the formation of lipid rafts and are suggested to modulate the chemical activity of cholesterol, which in turn could regulate its biosynthesis [31,32]. The strong stoichiometric complexation between NMEA and cholesterol demonstrated in the present study provides a potential model system for investigating the importance of lipid–lipid interactions in the formation and dynamics of rafts. Such specific complexes could be important in the cytoprotective and stress-combating actions of *N*-acylethanolamines.

Acknowledgements: This work was supported by a research grant from the Department of Science and Technology, Government of India to M.J.S.; M.R., R.K., R.K.K. and M.S.C. thank CSIR (New Delhi) for research fellowships. We thank Dr. M. Vairamani of IICT, Hyderabad for help in obtaining the FAB mass spectra and Chemical Computing Group, Montreal, Canada for providing the MOE program. We are grateful to Profs. K.C. Kumara Swamy and B.G. Maiya for scientific discussions.

References

[1] Schmid, H.H.O., Schmid, P.C. and Natarajan, V. (1990) Prog. Lipid Res. 29, 1–43.
[2] Schmid, H.H.O., Schmid, P.C. and Natarajan, V. (1996) Chem. Phys. Lipids 80, 133–142.
[3] Marsh, D. and Swamy, M.J. (2000) Chem. Phys. Lipids 105, 43–69.
[4] Hansen, H.S., Mosegaard, B., Hansen, H.H. and Petersen, G. (2000) Chem. Phys. Lipids 108, 135–150.
[5] Chapman, K.D. (2000) Chem. Phys. Lipids 108, 221–230.
[6] Epps, D.E., Schmid, P.C., Natarajan, V. and Schmid, H.H.O. (1979) Biochem. Biophys. Res. Commun. 90, 628–633.
[7] Epps, D.E., Natarajan, V., Schmid, P.C. and Schmid, H.H.O. (1980) Biochim. Biophys. Acta 618, 420–430.
[8] Devane, W.A., Hanus, L., Breuer, A., Pertwee, R.G., Stevenson, L.A., Griffin, G., Gibson, D., Mandelbaum, A., Etinger, A. and Mechoulam, R. (1992) Science 258, 1946–1949.
[9] Venance, L., Piomelli, D., Glowinski, J. and Giaume, C. (1995) Nature 376, 590–594.
[10] Schuel, H., Goldstein, E., Mechoulam, R., Zimmerman, A.M. and Zimmerman, S. (1994) Proc. Natl. Acad. Sci. USA 91, 7678–7682.
[11] Facci, L., Dal Toso, R., Romanello, S., Buriani, A., Skaper, S.D. and Leon, A. (1995) Proc. Natl. Acad. Sci. USA 92, 3376–3380.
[12] Chapman, K.D., Tripathy, S., Venables, B. and Desouja, A.D. (1998) Plant Physiol. 116, 1163–1168.
[13] Chapman, K.D., Venables, B.J., Markovic, R., Blair, R.W. and Bettinger, C. (1999) Plant Physiol. 120, 1157–1164.
[14] Ramakrishnan, M., Sheeba, V., Komath, S.S. and Swamy, M.J. (1997) Biochim. Biophys. Acta 1329, 302–310.
[15] Ramakrishnan, M. and Swamy, M.J. (1998) Chem. Phys. Lipids 94, 43–51.
[16] Ramakrishnan, M. and Swamy, M.J. (1999) Biochim. Biophys. Acta 1418, 261–267.
[17] Krishna, P., Prabhakar, S., Manoharan, M., Jemmis, E.D. and Vairamani, M. (1999) Chem. Commun. 1215–1216.
[18] Clark, J.H., Green, M., Madden, R., Reynolds, C.D., Miller, J.M. and Jones, T. (1984) J. Am. Chem. Soc. 106, 4056–4057.
[19] Brown, S.J. and Miller, M.J. (1987) J. Chem. Soc. Perkin Trans. II 1129–1132.
[20] Michaud, D.P., Kyranos, K.N., Brennan, T.F. and Vouros, P. (1990) Anal. Chem. 62, 1069–1074.
[21] Etter, M.C. (1990) Acc. Chem. Res. 23, 120–126.
[22] Feingold, L. (1993) Cholesterol in Membrane Models, CRC, Ann Arbor, MI.
[23] Ohwo-Rekilä, H., Ramstedt, B., Leppimäki, P. and Slotte, J.P. (2002) Prog. Lipid. Res. 41, 66–97.
[24] Brown, D.A. and Rose, J.K. (1992) Cell 68, 533–534.
[25] Brown, D.A. and London, E. (1998) Annu. Rev. Cell Dev. Biol. 14, 111–136.
[26] Simons, K. and Ikonen, E. (1997) Nature 387, 569–572.
[27] Sheets, E.D., Holowka, D. and Baird, B. (1999) Curr. Opin. Chem. Biol. 3, 95–99.
[28] Radhakrishnan, A. and McConnell, H.M. (1999) J. Am. Chem. Soc. 121, 486–487.
[29] Radhakrishnan, A. and McConnell, H.M. (1999) Biophys. J. 77, 1507–1517.
[30] Radhakrishnan, A., Li, X.-M., Brown, R.E. and McConnell, H.M. (2001) Biochim. Biophys. Acta 1511, 1–6.
[31] Radhakrishnan, A. and McConnell, H.M. (2000) Biochemistry 39, 8119–8124.
[32] Radhakrishnan, A., Anderson, T.G. and McConnell, H.M. (2000) Proc. Natl. Acad. Sci. USA 97, 12422–12427.